

Direction of Arrival Estimation in the presence of Scatterer in noisy environment

Tahniyat Aslam¹, Irfan Ahmed¹, Muhammad Imran Aslam^{1,*}, Syed M. Usman Ali¹, Tahir Malik¹

¹Department of Electronic Engineering, NED University of Engineering and Technology, Karachi, Pakistan
*corresponding author, E-mail: iaslam@neduet.edu.pk

Abstract

We present an algorithm to estimate direction of arrival (DOA) of an incoming wave received at an array antenna in the scenario where the incoming wave is contaminated by the additive white Gaussian noise and scattered by arbitrary shaped 3D scatterer(s). We present different simulation examples to show the validity of the proposed method. It is observed that the proposed algorithm is capable of closely estimating the DOA of an incoming wave irrespective of the shape of the scatterer provided the decision is made over multiple iterations. Moreover, presence of noise affects the estimate especially in the case of low signal-to-noise ratio (SNR) that gives a relatively large estimation error. However, for larger SNR the DOA estimation is primarily dependent on the scatterer only.

Keywords — Antenna Array, AWGN, Classical Beam forming, Direction of Arrival

1. Introduction

Array signal processing emerged in the last few decades as an active area of research. It is an important area in the field of signal processing, which uses antenna array to detect the useful signals while rejecting the interference and noise [1]. Direction-of-arrival estimation (DOA) plays an important role in array signal processing. The main purpose of the DOA algorithm is to estimate the direction of incoming signals while restraining the interference and noise. The accuracy of the estimate depends on the number of received signal samples. The benefit of using an array antenna is to enhance the resolution of multiple signals DOAs and has a better performance in signal detection and estimation than using a single antenna [2]. DOA estimation has several potential applications such as search and rescue, law enforcement and wireless emergency call locating etc. DOA estimation has considerable attention in wireless communication, radar system of commercial and military application and sonar system. The prime advantage of using DOA estimation algorithm is to improve the performance of an antenna by controlling the directivity of antenna to reduce the effects like interference, delay spread and multipath fading [3]. DOA estimation is also used to

increase the capacity and throughput of a network in wireless communication [4].

Several DOA estimation algorithms of narrowband signals are presented in the literature targeting the problem of DOA estimation in the presence of either noise [5-8] or in the presence of scatterer [9-12]. For the case of noise the DOA estimation is achieved by directly applying the algorithm on Uniform Linear Array without pre-processing techniques such as forward-backward averaging of the cross correlation of array output data or spatial smoothing. For the case of scatterer, spherical harmonics are used to remove the effects of scattered field. It has better realization of scattered field because the number of harmonics used is less and it also reduces the number of antenna elements in comparison of using cylindrical harmonics [10].

In this paper we address the problem of estimating the DOA in the situation where Additive White Gaussian Noise and 3D near zone scatterer are simultaneously present. The noise is independent of a signal and present at each antenna elements. The location of 3D scatterer is assumed to be known but its shape is not known. The effect of near zone scatterer is compensated by employing spherical harmonics expansions of unknown scattered field. A number of numerical experiments were conducted where multiple incident sources and multiple scatterers are present. For the purpose of simulation we choose ellipsoidal-shaped scatterer however there is no specific assumption on the shape of the scatterer in the algorithm which is shown by comparing results with a cubic-shaped scatterer in one of the examples. The simulation results show the performance of the proposed DOA estimation techniques.

Rest of the paper is organized as follows. Section 2 presents the proposed solution to find the DOA in the presence of both noise and scatterer. In section 3, different examples are presented to elaborate usability of the proposed method. Section 4 concludes the paper.

2. DOA Estimation

DOA estimation is a process for determining the signal of interest while rejecting the signal not of interest [13] using antenna arrays [14]. The presence of scattered field and noise in the received signals generate unintended copies of the signal that need to be rejected. We begin with the description of the considered environment and then present the proposed solution.

2.1. Environment Description

Consider uniform linear array (ULA) geometry with N identical x -directed dipole elements numbered from 1 to N as shown in Fig. 1. The array elements have a uniform spacing ‘ d ’ between them. Plane wave are used because source of incident wave is located sufficiently far away from the antenna elements [15]. Consider TM_x plane wave incident on an antenna array in x direction. Near field scatterers are also present, whose locations are known but geometries are unknown as shown in Fig. 1. The plane wave is scattered by the near-zone scatterer at location $r_s = (x_s, y_s, z_s)$ producing spherical waves/ harmonics. The plane wave and the scattered waves are incident on the n^{th} antenna element located at $r_n = (x_n, y_n, z_n)$. Therefore plane wave from far field region is desired signal and spherical waves due to near zone scatterer field are interfering signals. The total electric field at n^{th} antenna element is given by

$$E^t = E^{inc} + E^{sct} \quad (1)$$

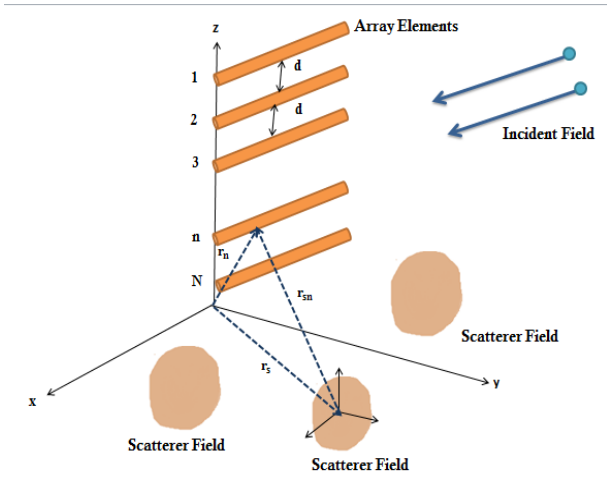


Figure 1: Incident Plane wave on N -element antenna array with arbitrary shaped near-zone Scatterer. Field at any antenna element is sum of both incident plane wave and the scattered waves.

An antenna array can be designed to estimate the direction of incoming signals based on samples of received signals. The accuracy of estimation method depends on the number of received signal samples K . It is also assumed that antenna and environment is stationary during K number of samples. The receiver is capable of measuring total voltage V^t at n^{th} antenna terminal that can be expressed as

$$V^t = V^{inc} + V^{sct} \quad (2)$$

Where, V^{inc} is the voltage due to incident field $E^{inc}(x)$ at n^{th} terminal, V^{sct} is the voltage due to scattered field arising from near zone scatterer $E^{sct}(x)$, V^t is the voltage at the n^{th} antenna terminal. If N_t is additive white Gaussian noise (AWGN), the output of receiver V^{rec} can be expressed as:

$$V^{rec} = V^t + N_t = V^{inc} + V^{sct} + N_t \quad (3)$$

2.2. Classical Method

Classical method for direction of arrival (DOA) estimation is based on the concept of beam forming. A commonly used classical method is Delay-and-sum method [16,17]. An array can steer beams through space and measure the output power. The direction from which maximum amount of power is obtained yields direction of arrival (DOA) estimation [18, 19]. Fig. 2, shows that the output signals ($z[k]$) is computed by using linear weights (w) combined with received data (x_k).

$$z[k] = \sum_{n=1}^N w_n x_n[k] = w^H x_k \quad (4)$$

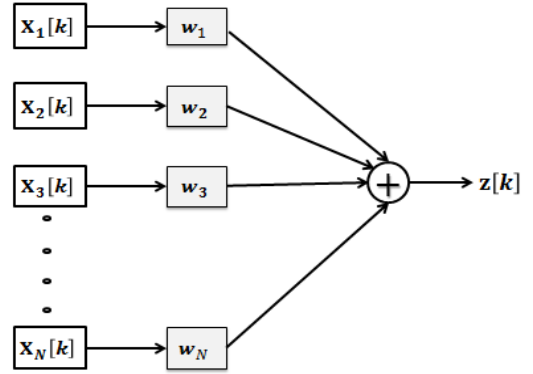


Figure 2: Illustration of Delay-And-Sum Method

The received data can be expressed as:

$$x[k] = \sum_{l=1}^L s_l[k] a(\varphi_l) + v[k] \quad (5)$$

Where, $x[k]$ is the k -th received sample for total L incident waves, $s_l[k]$ is the l -th incident wave, $a(\varphi_l)$ is a column of array manifold matrix relating the l -th incident wave to the receiver terminal, and $v[k]$ represents sample form AWGN. For known number of signal samples K , covariance matrix (R_{uu}) can be expressed as

$$R_{uu} = E[x_k x_k^H] \quad (6)$$

where $E[\cdot]$ represents expectation operator. In this case, the total output power of delay and sum method can be expressed as:

$$\begin{aligned} P(\theta) &= E[|z[k]|^2] = E[|w^H x_k|^2] \\ &= w^H E[x_k x_k^H] w = w^H R_{uu} w \end{aligned} \quad (7)$$

In classical beam forming, the signal power is measured over a angular region of interest by setting beam forming weights equal to steering weights $w = a(\theta)$ corresponding

to the particular direction. The output power is obtained as a function of angle of arrival as [20].

$$P(\theta) = w^H R_{uu} w = a(\theta) R_{uu} a(\theta)^H \quad (8)$$

The direction of arrival of the incident wave is taken as the direction corresponding to the maximum received power.

2.3. Proposed Solution

The total voltage at the output of the receiver V^{rec} is measured or known. In the absence of noise and scatterer the received signal is same as V^{inc} . However, actually the signal is corrupted by noise and scattered field. To remove the effect of AWGN from the total receiver voltage V^{rec} , we assumed that the total voltages received by incident field and scatterer field can be expressed as

$$X^{is} = V^{inc} + V^{sct} \quad (9)$$

This total voltage X^{is} is known or measured as mention earlier. The noise at each antenna terminal is independent from snapshot to snapshot and it is uncorrelated. But the signal remains same during each snapshot. The output of signal is given as

$$Y^{is} = X^{is} + V \quad (10)$$

Where, Y^{is} is the received output signal which is corrupted by Noise V . DOA estimation method uses sampled version of array output at k -th snapshot ($k = 1, 2, \dots, K$) is given by [21].

$$Y^{is}[k] = \sqrt{SNR} X^{is}[k] + V[k] \quad (11)$$

The key factor for this evaluation is Signal to Noise (SNR) of the environment surrounding the antenna arrays and incident sources, while the numbers of snapshots (K) is kept constant.

Next step is to remove the effect of scattering by using spherical harmonics. It is assumed that scatterers are exterior to array elements. It is to be noted that the incorrect assumption of letting $Y^{is} = V^{inc}$ not only causes errors in DOA estimate but may also give rise to false peaks in DOA spectrum. The linear equation for an array of N elements is given in [22].

Classical DOA estimation techniques are applied for $L^{(i)}$ number of sources and estimate their elevation $\theta = [\theta_1^{(i)}, \theta_2^{(i)}, \dots, \theta_L^{(i)}]$ at $i=0$. The algorithm is based on least square method with condition $M < N$. The total number of unknowns M is given as $M = L^{(i)} + 2SQ$. Where S is number of scatterer and Q is number of spherical harmonics. The incident voltage in each iteration is given by

$$V^{inc} = Y^{is} - V^{sct} \quad (12)$$

The incident voltage is used to find the elevation of desired incident sources and as iterative index is increases and algorithm is repeated until plot of convergence of DOA estimation is achieved.

3. Numerical Examples and Results

The electromagnetic simulations are carried out by using COMSOL multiphysics environment. In the considered scenarios we assumed (x -directed) horizontal half wave dipoles antenna elements of a uniform linear array. The radius of half wave dipole is $r_a = 0.001\lambda$. The operating frequency is 2.4GHz. The first element center is $(0,0,0)$ and its axis is along z direction as shown in Fig. 1. Two to three spherical harmonics will be sufficient to represent the field due to scatterer. Here we assumed that antenna and environment is stationary during a single sample. In real environment 3D scatterer can be approximated to a sphere, therefore spherical harmonics is used to remove the effects of scattered field. It has better realization of scattered field because the number of harmonics used is less and it also reduces the number of antenna elements in comparison of using cylindrical harmonics. In classical method, when the amplitude of DOA angle equals or exceeds to 40% of the maximum amplitude in spectrum the incident source is detected.

3.1. Case 1: Single Scatterer, Single Wave

The assumed geometry for case 1 is shown in Fig. 3, here number of scatterer $S=1$, scatterer in the form of ellipsoid (semi axis $a=0.5\lambda$, $b=0.5\lambda$ and $c=0.8\lambda$) and is located at $(0.1, -0.6, 3)\lambda$. The number of far ray elements $N=10$, the spacing between the elements is $d=0.5\lambda$. The incident wave $L=1$ and the elevation of incident wave is $\theta = 75^\circ$. Gaussian noise is added at each antenna element and it is assumed that noise is complex and uncorrelated.

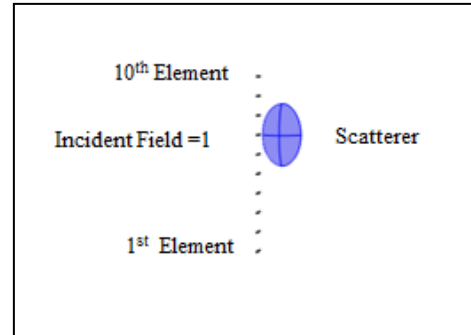


Figure 3: Geometric setup for case 1

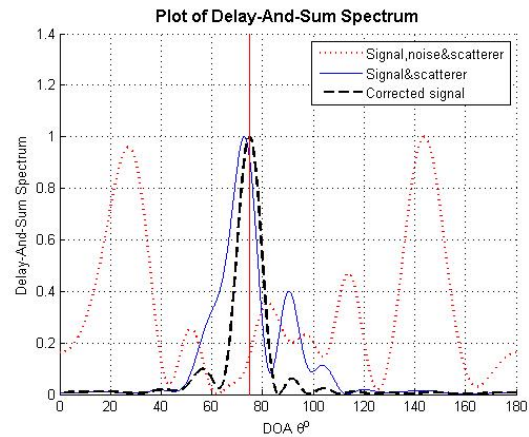


Figure 4: DOA spectrum for case 1

The DOA spectrum obtained in this case is shown in Fig. 4. Due to the presence of noise and scatterer, the peak is shifted thereby introducing errors. Moreover three spurious DOA peaks at 27.1° , 113.8° and 143.7° are also detected. When the noise is removed the initial algorithm of delay and sum estimates incident wave DOA $\theta_1^{(0)} = 72.8^\circ$ and one spurious DOA at 90.4° is also detected at SNR= 10 dB. The corrected spectrum suppresses the spurious peak and gives desired DOA estimation. The convergence of $\theta^{(i)}$ to $\theta^{(l)} = 74.8^\circ$ using spherical harmonics $Q=3$ as shown in Fig. 5.

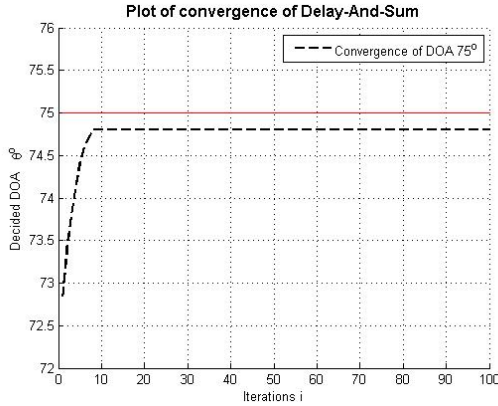


Figure 5: Convergence of decided $\theta^{(l)}$ for case 1

The effect of noise in the DOA estimation is elaborated in Fig. 6 that shows the plot of DOA estimation with respect to SNR. Relatively large estimation error is observed in the low SNR regime. As SNR increases the error tends to reduce and eventually the DOA estimation is converged to the case of scatterer only (i.e. no noise). The result is quite intuitive as in case of low SNR the effect of noise is dominating the signal thereby producing larger error. As SNR is increased the effect of noise reduces in comparison to the signal and the decision is mainly dependent on the scattering effect.

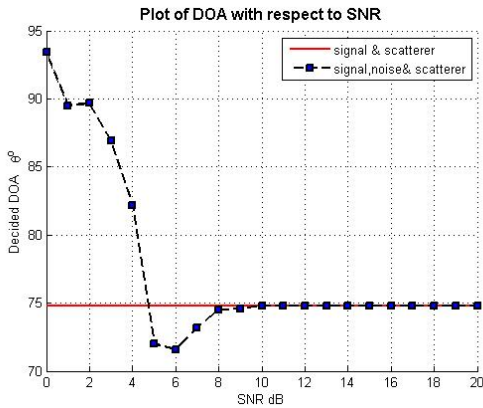


Figure 6: Plot of DOA with respect to SNR for case 1

3.2. Case 2(a): Single Scatterer, Two Waves

In case 2, we use two different scatterer geometries (a) cube (b) ellipsoid with a approximately same size and same location to show that the proposed algorithm is applicable to any 3D geometry. The simulation environment for case 2(a) is shown in Fig. 7. The case 2(a) is similar to the case 1

except that two incident waves ($L=2$) with elevation angles $\theta_1 = 80^\circ$ and $\theta_2 = 120^\circ$ are used. The number of scatterer $S=1$ and it is in the form of cube with side length λ and is located at $(0.2, -0.6, 2.5)\lambda$. The number of array elements $N=10$ and the spacing between the element is $d=0.5\lambda$. The signal is contaminated with AWGN which is uncorrelated at each antenna element,

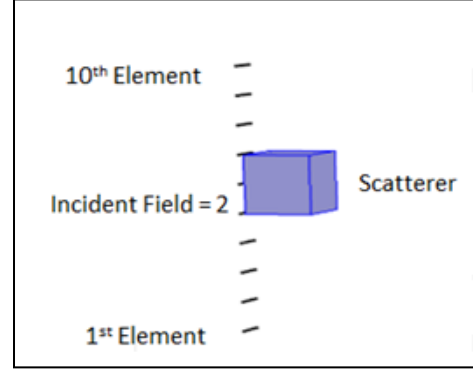


Figure 7: Geometric setup for case 2(a)

The presence of noise and scatterer shifts the peak and introduces five spurious DOAs at 69.0° , 84.3° , 98.2° , 116.7° and 158.7° . When the noise is removed, the initial algorithm of delay and sum estimates incident wave DOA $\theta_1^{(0)} = 79.8^\circ$ and $\theta_2^{(0)} = 119.6^\circ$ as shown in Fig. 8. One spurious DOA 63.4° is also detected at SNR = 10 dB. The corrected spectrum suppresses the spurious peak and gives desired DOA estimation.

The convergence of first decided DOA is $\theta_1^{(i)}$ to $\theta_1^{(l)} = 79.2^\circ$ and the convergence of second decided DOA is $\theta_2^{(i)}$ to $\theta_2^{(l)} = 119.7^\circ$ as shown in Fig. 9 using $Q=3$ Spherical harmonics. The Fig. 10 shows the plot of decided DOA with respect to SNR. In this case when the scatterer is present, the first decided DOA is detected at 79.2° and the second decided DOA is detected at 119.7° . But in the presence of noise and scatterer, the algorithm gives the same results at high SNR for both decided DOAs.

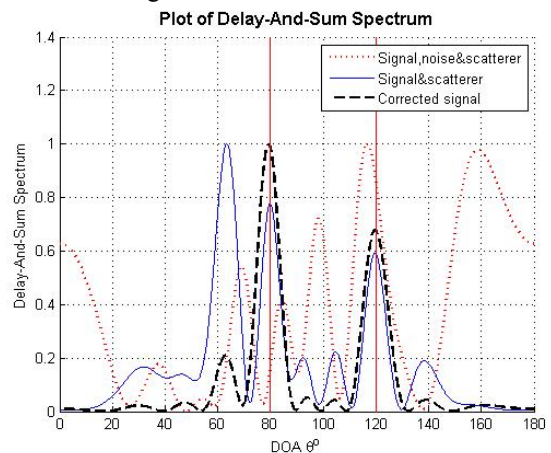


Figure 8: DOA spectrum for case 2(a)

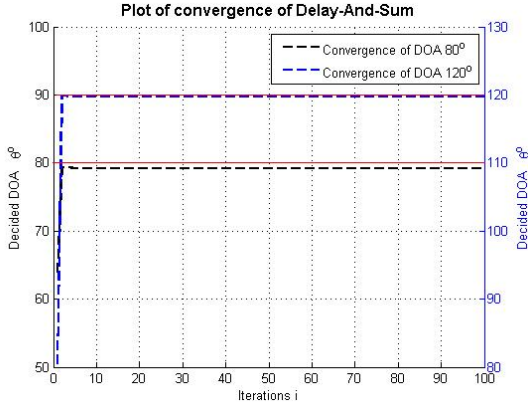


Figure 9: Convergence of decided $\theta^{(l)}$ for case 2(a)

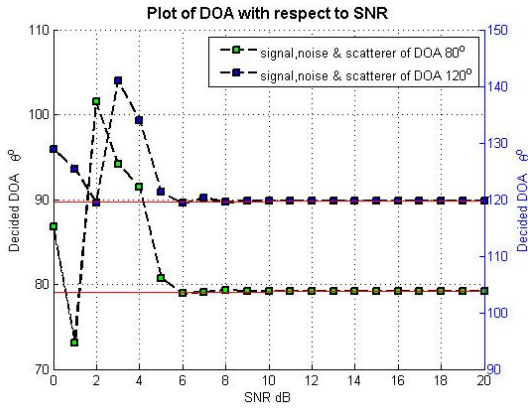


Figure 10: Plot of DOA with respect to SNR for case 2(a)

3.3. Case 2(b): Single Scatterer, Two Waves

The case 2(a) is repeated with different shape of scatterer. Here the scatterer is in the form of ellipsoid (semi axis $a=0.5\lambda$, $b=0.5\lambda$ and $c=0.8\lambda$) and it is located at same location as in previous case at $(0.2, -0.6, 2.5)\lambda$ as shown in Fig. 11. Here the number of incident wave $L=2$ and the elevation of incident wave is $\theta_1 = 80^\circ$ and $\theta_2 = 120^\circ$. The number of array elements $N=10$ and the spacing between the element is $d=0.5\lambda$. Here Gaussian noise is added and it is assumed that noise is uncorrelated.

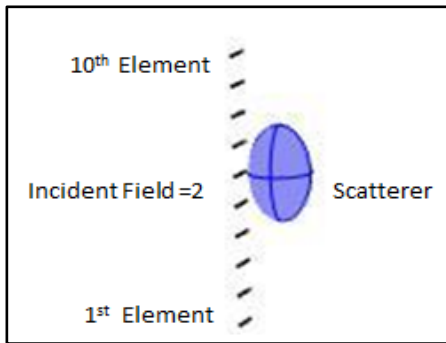


Figure 11: Geometric setup for case 2(b)

In the presence of noise, the peak is shifted and introducing errors, four spurious DOAs at 39.9° , 83.7° , 120.0° and 140.2° . when the noise is removed, the initial algorithm of delay and sum estimates incident wave DOA $\theta_1^{(0)} = 78.9^\circ$ and $\theta_2^{(0)} = 120.0^\circ$ as

shown in Fig. 12. One spurious DOA 63.4° is also detected at SNR = 10dB. The corrected spectrum suppresses the spurious peak and gives desired DOA estimation.

The convergence of first decided DOA is $\theta_1^{(l)}$ to $\theta_1^{(l)} = 79.0^\circ$ and the convergence of second decided DOA is $\theta_2^{(l)}$ to $\theta_2^{(l)} = 119.6^\circ$ as shown in Fig. 13 using $Q = 3$ Spherical harmonics. The Fig. 14 shows the plot of decided DOA with respect to SNR. In this case when the scatterer is present, the first decided DOA is detected at 79.0° and the second decided DOA is detected at 119.6° . But in the presence of noise and scatterer, the algorithm gives the same results at high SNR for both decided DOAs.

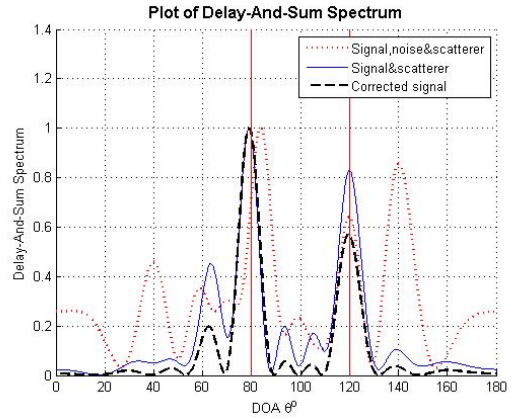


Figure 12: DOA spectrum for case 2(b)

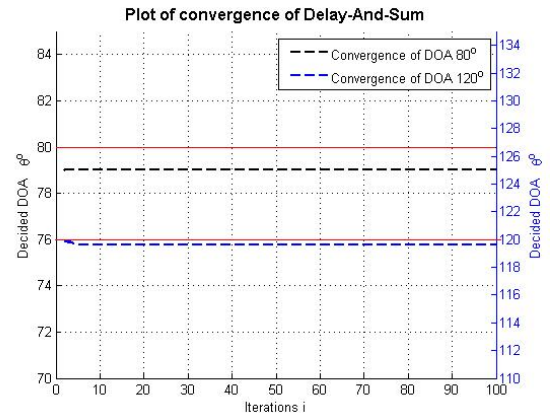


Figure 13: Convergence of decided $\theta^{(l)}$ for case 2(b)

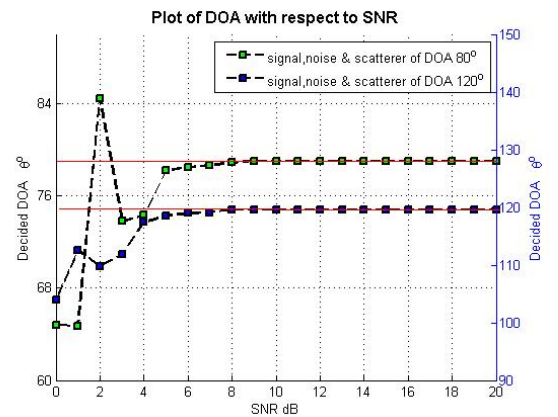


Figure 14: Plot of DOA with respect to SNR for case 2(b)

3.4. Case 3: Two Scatterers, Single Wave

The setup of case 3 is shown in Fig. 15. This case is more complex because the number of array elements are increased to $N=20$ and the spacing between the element is $d=0.25\lambda$. Here number of scatterer $S=2$. Both scatterer are in the form of sphere (radius = 0.5λ) and are located at $(-0.2, -0.6, 4)\lambda$ and $(-0.2, -0.6, 1)\lambda$. There is one incident wave ($L=1$) and the elevation of incident wave is $\theta_1 = 95^\circ$. Gaussian noise is added and it is assumed that noise is uncorrelated.

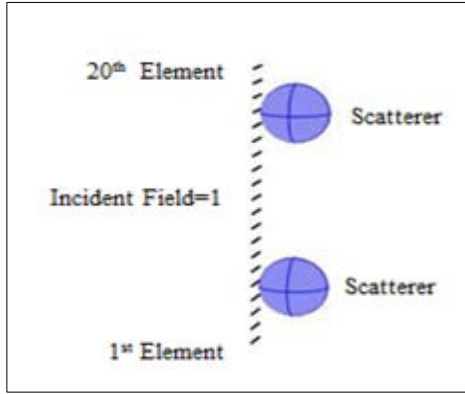


Figure 15: Geometric setup for case 3

Fig. 16 shows that in the presence of noise, the peak is shifted and introducing errors, two spurious DOAs 60.2° and 85.4° are also detected. When the noise is removed the initial algorithm of delay and sum estimates incident wave DOA at $\theta_1^{(0)} = 94.6^\circ$. One spurious DOA at 119.8° is also detected at SNR=10dB.

The convergence of decided DOA is $\theta^{(l)}$ to $\theta^{(l)} = 95.1^\circ$ as shown in Fig. 17 using $Q = 2$ Spherical harmonics. The Fig. 18 shows the plot of decided DOA with respect to SNR. In this case when the scatterer is present, decided DOA is detected at 95.1° . But in the presence of noise and scatterer, the algorithm gives the same results in high SNR.

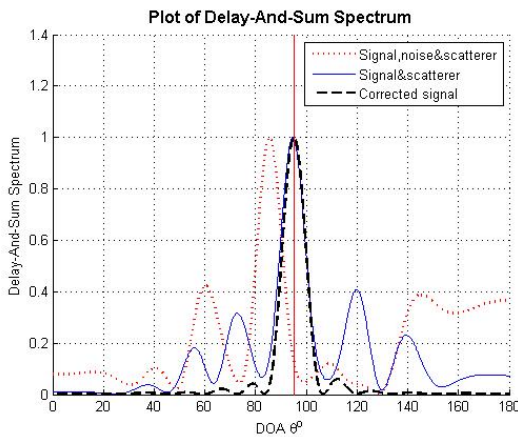


Figure 16: DOA spectrum for case 3

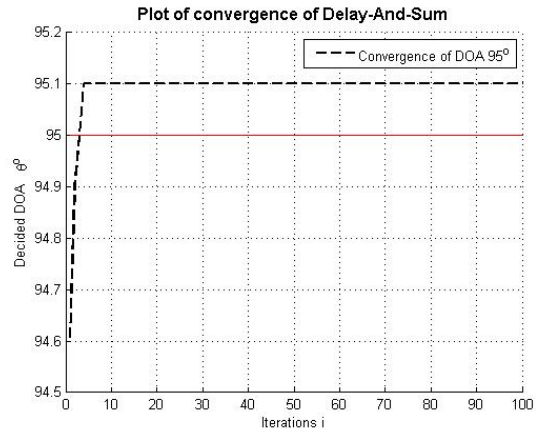


Figure 17: Convergence of decided DOA $\theta^{(l)}$ for case 3

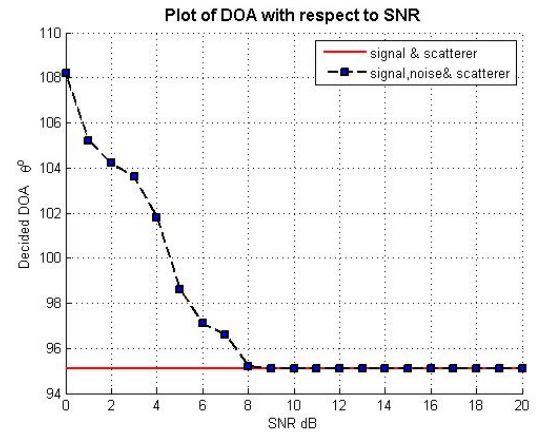


Figure 18: Plot of DOA with respect to SNR for case 3

3.5. Case 4: Two Scatterers, Two Waves

The geometry of case 4 is shown in Fig. 19. Here number of scatterer $S=2$. One scatterer is in the form of ellipsoid (semi axis $a=0.4\lambda$, $b=0.5\lambda$ and $c=0.7\lambda$) and is located at $(0.1, -0.6, 4)\lambda$. Another scatterer is in the form of sphere (radius = 0.5λ) and is located at $(-0.1, -0.6, 1.5)\lambda$. The number of array elements $N=20$ and spacing between the element is $d=0.25\lambda$. The incident wave $L=2$ and the elevation of incident wave is $\theta_1 = 65^\circ$ and $\theta_2 = 120^\circ$. Gaussian noise is added and it is assumed that noise is uncorrelated.

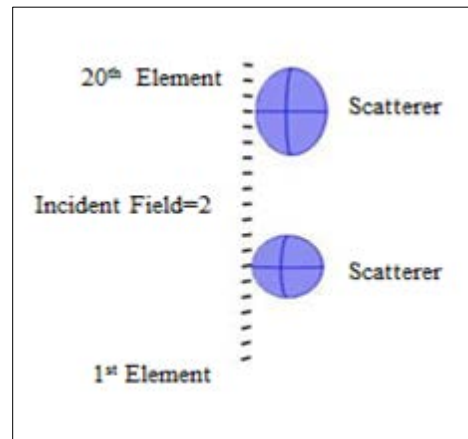


Figure 19: Geometric setup for case 4

Fig. 20 shows that in the presence of noise, the peak is shifted and introducing errors, five spurious DOAs at 35.6° , 53.6° , 78.0° , 104.1° and 126.8° are detected. When the noise is removed the initial algorithm of delay and sum estimates incident wave DOA $\theta_1^{(0)} = 62.3^\circ$ and $\theta_2^{(0)} = 120.5^\circ$. Two spurious DOAs 87.5° and 103.3° are also detected at SNR= 10dB. The corrected spectrum suppresses the spurious peak and gives desired DOA estimation.

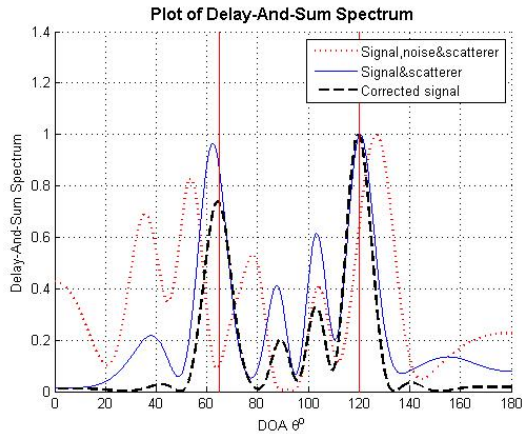


Figure 20: DOA spectrum for case 4

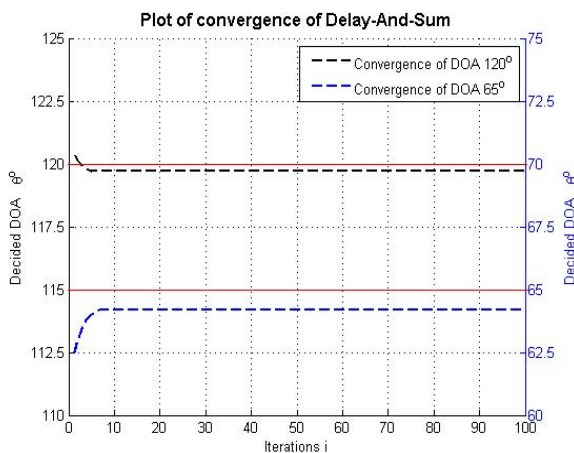


Figure 21: Convergence of decided DOA $\theta^{(l)}$ for case 4

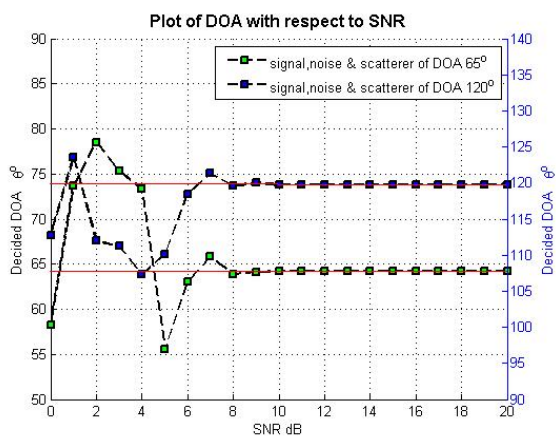


Figure 22: Plot of DOA with respect to SNR for case 4

The convergence of first decided DOA is $\theta_1^{(l)}$ to $\theta_1^{(l)} = 64.2^\circ$ and the second decided DOA is from convergence of $\theta_2^{(l)}$ to $\theta_2^{(l)} = 119.7^\circ$ as shown in Fig. 21 using $Q = 2$ Spherical harmonics. The Fig. 22 shows the plot of decided DOA with respect to SNR. In this case when the scatterer is present, the first decided DOA is detected at 64.2° and the second decided DOA is detected at 119.7° . But in the presence of noise and scatterer, the algorithm gives the same results at high SNR for both decided DOAs.

4. Conclusions

An iterative algorithm for DOA estimation is presented in the case where Additive White Gaussian Noise (AWGN) and 3D scatterer(s) are simultaneously present. Although all the simulations are performed with the cubic, spherical, or ellipsoidal scatterer, the algorithm imposes no condition on the shape of the scatterer. However the location of the scatterer must be known. The convergence of DOA is achieved iteratively and algorithm is repeated until the correct (converged) DOA is achieved. A number of numerical experiments were conducted where multiple incident sources and multiple scatterers are present. Where noise is assumed to be independent and present at each antenna terminal. It is also assumed that signal remain same at each sample. SNR directly affect the performance of DOA estimation especially in the low SNR regime. It is observed that the algorithm is capable of closely estimating the DOA in the presence of noise and scatterers.

References

- [1] Krim, Hamid, and Mats Viberg. "Two decades of array signal processing research: the parametric approach." *IEEE signal processing magazine* 13.4 (1996): 67-94.
- [2] Van Trees, Harry L. *Detection, estimation, and modulation theory, optimum array processing*. John Wiley & Sons, 2004.
- [3] Abdalla, Moustafa M., Moustafa B. A. Buitbel, and Mohamed A. Hassan. "Performance evaluation of direction of arrival estimation using MUSIC and ESPRIT algorithms for mobile communication systems." *Wireless and Mobile Networking Conference (WMNC), 2013 6th Joint IFIP*. IEEE, 2013.
- [4] Foutz, Jeffrey, Andreas Spanias, and Mahesh K. Banavar. "Narrowband direction of arrival estimation for antenna arrays." *Synthesis Lectures on Antennas* 3.1 (2008): 1-76.
- [5] Khmou, Youssef, Said Safi, and Miloud Frikel. "Comparative study between several direction of arrival estimation methods." *Journal of Telecommunications and Information Technology* (2014).
- [6] Wang, Haiqiang, Jianguo Huang, and Wei Gao. "DOA estimation for coherent sources in the presence of unknown correlated noise." *Signal Processing, Communication and Computing (ICSPCC), 2012 IEEE International Conference on*. IEEE, 2012.

- [7] Xiao-guang, Wu, and Guo Tian-wen. "Direction of arrival parametric estimation and simulation based on MATLAB." *Proceedings of the 2011, International Conference on Informatics, Cybernetics, and Computer Engineering (ICCE2011) November 19–20, 2011, Melbourne, Australia*. Springer Berlin Heidelberg, 2011.
- [8] Godara, Lal C. "Application of antenna arrays to mobile communications. II. Beam-forming and direction-of-arrival considerations." *Proceedings of the IEEE* 85.8 (1997): 1195-1245.
- [9] Ahmed, Irfan, and Perger, Warren "Direction Finding in the Presence of Near Zone Resonant Size Scatterers." *Progress In Electromagnetics Research B* 56 (2013): 219-234.
- [10] Horiki, Yasutaka, and Edward H. Newman. "A self-calibration technique for a DOA array with near-zone scatterers." *IEEE transactions on antennas and propagation* 54.4 (2006): 1162-1166.
- [11] Ahmed, Irfan and Perger, Warren, "Effects of ground on antenna mutual impedance for DOA estimation using dipole arrays," *Progress In Electromagnetics Research C*, Vol. 46, 179-185, 2014.
- [12] Ahmed, Irfan; Perger, Warren, and Zekavat, Seyed A.; "Effects of Ground Constituent Parameters on Array Mutual Coupling for DOA Estimation," *International Journal of Antennas and Propagation*, vol. 20 11, Article ID 425913, 5 pages, 2011.
- [13] Balanis, Constantine A., and Panayiotis I. Ioannides. "Introduction to smart antennas." *Synthesis Lectures on Antennas* 2.1 (2007): 1-175.
- [14] Balanis, Constantine A. *Antenna theory: analysis and design*. John Wiley & Sons, 2016.
- [15] Chen, Zhizhang, Gopal Gokeda, and Yiqiang Yu. *Introduction to Direction-of-arrival Estimation*. Artech House, 2010.
- [16] Badawy, Ahmed, et al. "A simple localization scheme." *arXiv preprint arXiv:1409.5744* (2014).
- [17] Schell, Stephan V., and William A. Gardner. "18 High-resolution direction finding." *Handbook of statistics* 10 (1993): 755-817.
- [18] Liberti, Joseph C., and Theodore S. Rappaport. *Smart antennas for wireless communications: IS-95 and third generation CDMA applications*. Prentice Hall PTR, 1999.
- [19] Elkamchouchi, Hassan, and Mohamed Abd Elsalam Mofeed. "Direction-of-arrival methods (DOA) and time difference of arrival (TDOA) position location technique." *Radio Science Conference, 2005. NRSC 2005. Proceedings of the Twenty-Second National*. IEEE, 2005.
- [20] Bhuiya, S. N., F. Islam, and M. A. Matin. "Analysis of Direction of arrival techniques using uniform linear array." *International Journal of Computer Theory and Engineering* 4, no. 6 (2012): 931.
- [21] Tuncer, T. Engin, and Benjamin Friedlander, eds. *Classical and modern direction-of-arrival estimation*. Academic Press, 2009.
- [22] Balanis, Constantine A. *Advanced engineering electromagnetics*. John Wiley & Sons, 2012.